Impact of Mg Doping on Performances of CuGaO2 Based p-Type Dye-Sensitized Solar Cells

ARTICLE *in* THE JOURNAL OF PHYSICAL CHEMISTRY C · JANUARY 2014

Impact Factor: 4.77 · DOI: 10.1021/jp407233k

9 AUTHORS, INCLUDING:

Adèle Renaud
Arizona State University
8 PUBLICATIONS **148** CITATIONS
SEE PROFILE

Laurent Cario
Institut des Materiaux Jean Rouxel
150 PUBLICATIONS **1,361** CITATIONS
SEE PROFILE

Philippe Deniard
French National Centre for Scientific Research
105 PUBLICATIONS **3,054** CITATIONS
SEE PROFILE

Eric Gautron
Institut des Materiaux Jean Rouxel
75 PUBLICATIONS **510** CITATIONS
SEE PROFILE

THE JOURNAL OF PHYSICAL CHEMISTRY C

Article

pubs.acs.org/JPCC

Impact of Mg Doping on Performances of $CuGaO_2$ Based p-Type Dye-Sensitized Solar Cells

Adèle Renaud,[†] Laurent Cario,*[,†] Philippe Deniard,[†] Eric Gautron,[†] Xavier Rocquefelte,[†] Yann Pellegrin,[‡] Errol Blart,[‡] Fabrice Odobel,[‡] and Stéphane Jobic*[,†]

[†]Institut des Matériaux Jean Rouxel, Université de Nantes, CNRS, 2 rue de la Houssinière, BP 32229, 44322 Nantes, Cedex 03, France

[‡]Université LUNAM, Université de Nantes, CNRS, Chimie et Interdisciplinarité: Synthèse, Analyse, Modélisation (CEISAM), UMR 6230, 2 rue de la Houssinière, 44322 Nantes, Cedex 03, France

ABSTRACT: p-Type dye solar cells (p-DSSCs) have been receiving much attention due to their potential role in the elaboration of future tandem dye solar cells with a photoanode and a photocathode built upon n-type and a p-type semiconductors, respectively. So far, NiO appears as the most widely used semiconductor in p-DSSCs. Yet this material suffers from several drawbacks, e.g., a low electrical conductivity and a low redox potential that limit the photovoltaic performances. In that framework, delafossite compounds may be regarded as appropriate substitutes of nickel oxide in relation to their intrinsic optoelectronic properties. Here we report on the nanostructuration of $CuGaO_2$ and its Mg doped derivatives via hydrothermal conditions with Pluronic P123 as surfactant. It appears that a low amount of magnesium helps in preparing samples with higher specific surface areas and stimulates enhanced conversion efficiencies. Beyond a given Ga/Mg substitution rate, a new $Cu_{1-x}(Ga,Mg)O_2$ phase is formed that contains a large amount of Cu vacancies and of structural defects. This new phase shows lower photovoltaic performances compared to those for slightly doped derivatives which suggests that Cu vacancies and/or structural defects limit the mean free path of holes within the photocathode.

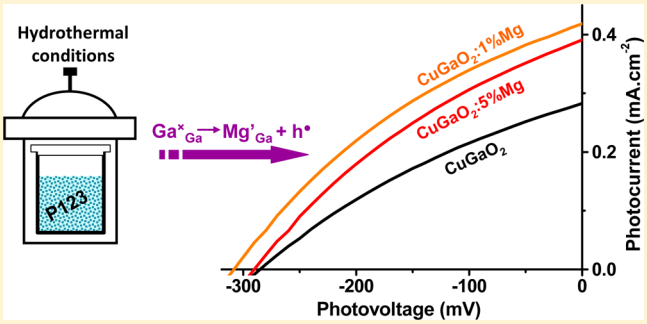

INTRODUCTION

Solar cells based on the sensitization of a p-type semiconductor are of growing interest to researchers.[1−7] The development of such devices appears as the mandatory step to achieve tandem dye-sensitized solar cells (t-DSSCs) with a photoanode built upon a conventional n-type semiconductor (n-SC, e.g., TiO_2 and ZnO)[8,9] and a photocathode built upon a p-type semiconductor (p-SC, e.g., NiO and CuO),[1,2,10] both electrodes being sensitized by two distinct dyes. The fabrication of such devices would open up the door to higher efficiencies in the conversion of sunlight into electrical power compared to n-DSSCs alone as demonstrated by He et al.,[11] Odobel et al.,[12] and Nattestad et al.[13] Unfortunately, p-DSSCs performances are currently very low compared with those of n-DSSCs, and intensive work has to be dedicated to the quest to find new nanostructurated p-SCs to favor higher open-circuit voltage (V_{OC}), short-circuit current (J_{SC}), and fill factor (ff).[14] To date, the most frequently used p-SC in p-DSSCs remains by far NiO with a common conversion efficiency (η) of a few tens of a percent. Nevertheless, it is worth noticing that a real breakthrough was recently discovered by Powar et al.[15] where NiO is coupled with the outstanding PMI-6T-TPA dye as a sensitizer and tris(1,2-diaminoethane)cobalt(II/III) complexes as a redox mediator to reach a η value of 1.3%. Moreower, new p-SCs were recently explored to replace NiO and significant success were achieved with delafossites.[3−6,16,17] The limited performances of NiO-based solar cells were so far in part attributed to a too high energy position of the top of its valence band. In that framework, we have embarked recently on the synthesis of p-type $CuGaO_2$-delafossite nanoparticles in ethylene glycol (EG) mediated hydrothermal conditions.[18] Namely electrochemical impedance spectroscopy (EIS) measurements on NiO and $CuGaO_2$ samples evidenced an increase of the flat band potentials (FBP) by almost 200 mV shifting from the binary to the ternary compounds. Unfortunately, this significant enhancement of the FBP does not go along with an increase of the p-DSSCs performances, owing to a still low short circuit photocurrent (Jsc) likely due to unoptimized p-SC/dye and dye/mediator interfaces favoring counter-productive reactions. This may also be associated with a relatively low absorbance of the photocathode suggesting that the size of prepared $CuGaO_2$ particles is still too large leading to low specific surface area and finally a low amount of adsorbed dyes on its surface. An increase of J_{SC} in $CuGaO_2$ based DSSCs appears therefore as the key point to outperform NiO based cells. For that purpose, it is crucial to obtain smaller

Received: July 22, 2013
Revised: December 10, 2013
Published: December 11, 2013

   dx.doi.org/10.1021/jp407233k | J. Phys. Chem. C 2014, 118, 54−59

Table 1. Real Chemical Compositions of $CuGaO_2$, $CuGaO_2$:1%Mg, $CuGaO_2$:5%Mg, and $CuGaO_2$:10%Mg Samples Deduced from ICP Measurements

sample	Cu/Ga	Mg/Ga	Mg/(Mg+Ga)	composition
$CuGaO_2$−P123	0.99	0	0	$CuGaO_2$
$CuGaO_2$:1%Mg	0.99	0.007	0.007	$CuGa_{0.993}Mg_{0.007}O_2$
$CuGaO_2$:5%Mg	0.92	0.049	0.047	$Cu_{0.86}Ga_{0.953}Mg_{0.047}O_2$
$CuGaO_2$:10%Mg	0.89	0.058	0.055	$Cu_{0.84}Ga_{0.945}Mg_{0.055}O_2$

nanoparticle size in a reproductive manner. A second option to favor the flow of injected charges (and to limit consequently the electron−hole recombination) consists of increasing the conductivity of $CuGaO_2$ by doping. In that framework, the substitution of Mg^{2+} for Ga^{3+} naturally emerges. In this work, first we report on the use of a P123 triblock copolymer as a templating agent to favor the nanostructuration of $CuGaO_2$ and Mg doped $CuGaO_2$ materials, and second we discuss the impact of the nanostructuration and the chemical composition of the as-obtained p-SCs on the photovoltaic performances of p-DSSCs.

EXPERIMENTAL SECTION

Synthesis of $CuGaO_2$ and $CuGaO_2$:Mg. Materials were prepared according to the slightly modified chemical route initially set up by Srinivasan et al.[18] Namely, $CuGaO_2$ (hereafter labeled $CuGaO_2$−P123) was synthesized in hydrothermal conditions (i.e., 70% filled Teflon bomb sealed in an autoclave) at 190 °C for 56 h from 1 mmol copper and gallium nitrates ($Cu(NO_3)_2{\cdot}3H_2O$, Alfa Aesar, 98% and hydrated $Ga(NO_3)_3$ from Alfa Aesar, 99.9%) and 3.6 g (i.e., 0.6 mmol) of Pluronic P123 surfactant ($HO(CH_2CH_2O)_{20}(CH_2CH(CH_3)O)_{70}(CH_2CH_2O)_{20}H$, Aldrich) in a 21 mL aqueous solution adjusted at pH of 5.15 with a 1 M NaOH solution. The as-synthesized samples might contain low amounts of Cu_2O and/or Cu as side products. They were removed via rinsing in ammonia, nitric acid, and distilled water before characterization and use as photocathode. The synthesis of Mg doped $CuGaO_2$ samples was carried on in similar conditions where $Mg(NO_3)_2{\cdot}6H_2O$ is partially substituted for $Ga(NO_3)_3{\cdot}xH_2O$ (prior to mixing of nitrate solutions, x was determined by pHmetry). In the following, Mg percentages in $CuGaO_2$:p%Mg samples correspond to the nominal Mg/(Mg + Ga) precursor rate introduced in the Teflon bomb. Table 1 gathers the correspondence between the targeted and the real Mg/Ga ratios in $CuGaO_2$:Mg compounds on the basis of inductively coupled plasma optical emission measurements.

Physical Property Measurements. Powder X-ray diffraction patterns were recorded in Bragg−Brentano geometry on a D8 Bruker diffractometer equipped with a front germanium monochromator (Cu K-L_3 radiation) and a LynxEye PSD detector. Transmission electron microscopy was performed on a Hitachi H-900NAR (accelerating voltage of 300 kV, Scherzer resolution of 0.18 nm). Prior to examination, the samples were ground in ethanol and dispersed ultrasonically. A drop of the suspension was deposited on a copper grid previously covered with a thin holey carbon film. Scanning electron microscopy images were collected on a JEOL7600F apparatus on powder spread on a carbon tape pasted over a copper metal sample holder. Brunauer−Emmett−Teller (BET) analyses were done in a micrometrics ASAP 2010BET. Induced coupled plasma/optical emission spectroscopy (ICP-OES) measurements were carried out on a iCAP 6300 (Thermo Scientific) on $CuGaO_2$ and Mg doped $CuGaO_2$ materials dissolved in HNO_3 solution.

Fabrication of Photocathode and Photovoltaic Characterization. Namely, 0.5 g of powdered materials was mixed in 10 mL of absolute ethanol by ball milling. Then, this mixture was poured dropwise in 3.32 mL of Terpineol and 1.66 mL of ethanol/ethylcellulose (9:1) solution. Ethanol was removed with a rotary evaporator resulting in a paste with a suitable viscosity to be deposited on FTO-coated glass substrates (Pilkington TEC8, 8 Ω/sq) by serigraphy. A double-pass deposition separated by an intermediate drying step at 80 °C in an oven was needed to get 4 μm thick crack-free inorganic layers after heating in air at 350 °C for 30 min. Then, films were dipped for 48 h in a PMI-NDI dyad solution,[10] and DSSCs were assembled; that is, the photocathode/polymer spacer (25 μm, Surlyn)/platinum-coated FTO glass were stacked together and sealed by heating under pressure. The interspaced layer was filled via a drilled hole (via vacuum backfilling technique[19]) by an electrolyte, a mixture of 0.1 M tris(4,4′-bis-tert-butyl-2,2′-bipyridine)cobalt(II/III) and 0.1 M $LiClO_4$ in propylene carbonate. The hole was isolated with a glass disk by sealing with a hot melt polymer gasket (60 μm, Surlyn). Solar cell performances were recorded on a Keithley model 2420 digital source meter under AM 1.5G simulated sunlight (1000 mW/cm^2). The exact amount of dye loaded on each film was determined by UV−visible absorption after desorption of the dye in a 0.1 M of NaOH in DMF bath. NB: Platinized FTO glasses were used here as counter electrodes. Nevertheless, others materials such as graphene-based anodes would have likely to be privileged in the near future as suggested by Kavan et al. and Hao et al. when Co-based redox mediators are used.[20,21]

RESULTS AND DISCUSSION

The synthesis of $CuGaO_2$ nanoparticles using ethylene glycol (EG) as reducing agent to stabilize Cu^+ under hydrothermal conditions was reported a few years ago by Srinisasan et *al.*.[18] These nanoparticles with a hexagonal plate-like shape (300 nm side, 20 nm thick) lead to powder samples (hereafter labeled $CuGaO_2$-EG) with specific surface area (SSA) of 30 m^2/g. Their use in a p-DSSC device yielded photovoltaic performances of 0.015% with a *V*oc and a *J*sc of 375 mV and 0.12 mA cm^{-2}, respectively, with PMI-NDI as push−pull sensitizer[12,22] and tris(4,4′-bis-tert-butyl-2,2′-bipyridine) cobalt (Co^{2+}/Co^{3+})[22] as redox mediator. Compared with NiO based devices, conversion efficiency was lower, mainly due to a too low short circuit current density (0.12 vs 1.2 mA cm^{-2}) but the open circuit voltage was enhanced (375 vs 285 mV) as anticipated from the flat band measurements.[4] In order to increase *J*sc via the prepararion of more nanostructurated materials, we have explored a new chemical route for $CuGaO_2$ and its Mg doped derivatives based on the use of a templating agent, namely, the template triblock copolymer Pluronic P-123, commonly

dx.doi.org/10.1021/jp407233k | J. Phys. Chem. C 2014, 118, 54−59

employed as micelles in solution to produce structured mesoporous materials.[23,24]

The X-ray diffraction (XRD) pattern of $CuGaO_2$ sample synthesized with P-123 ($CuGaO_2$−P123) is depicted in Figure 1 and compared with the $CuGaO_2$-EG reference sample.[14] As

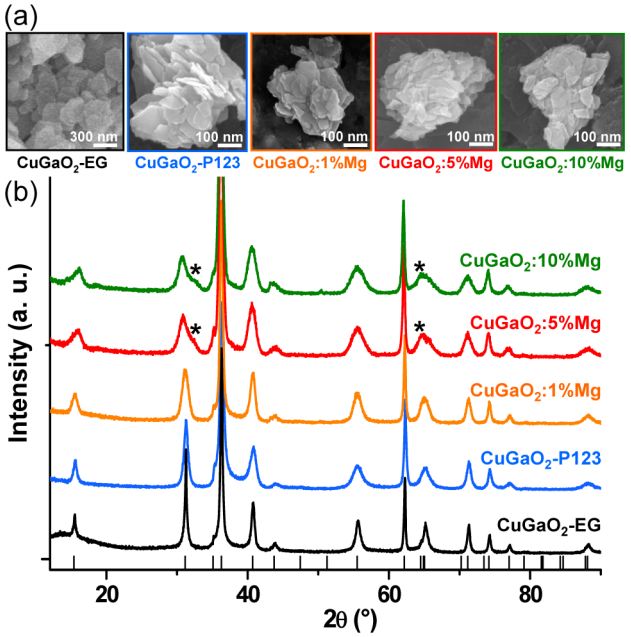

Figure 1. (a) SEM photographs of $CuGaO_2$-EG, $CuGaO_2$−P123 (sample with the higher SSA), $CuGaO_2$:1%Mg, $CuGaO_2$:5%Mg, and $CuGaO_2$:10%Mg and (b) corresponding XRD patterns. Sticks correspond to the diffraction peaks location of the $CuGaO_2$-3R form (ICSD file no. 60846). Asterisks correspond to additional peaks at ∼32° and ∼64° in 2θ detected for $CuGaO_2$:5%Mg and $CuGaO_2$:10% Mg.

expected, both diagrams are comparable and display the diffraction peaks of the 3R allotropic form of $CuGaO_2$.[25,26] Clearly, going from $CuGaO_2$-EG to $CuGaO_2$−P123, a decrease of crystallite size is observed as illustrated by a widening of the diffraction peaks. This can suggest an overall reduction of the particles size of $CuGaO_2$−P123 which is confirmed by comparing scanning electron microscopy photographs of both $CuGaO_2$ samples (mean ⌀ ≈ 200 nm, e ≈ 5 nm for $CuGaO_2$−P123 according to Figure 1a). Concomitantly the best specific surface areas (SSA) measured by the Brunauer−Emmet−Teller method can be significantly increased from 30 m^2/g in $CuGaO_2$-EG to 42 m^2/g in $CuGaO_2$−P123. However, we observed a lack of reproducibility in the synthesis of $CuGaO_2$−P123 (as well as for $CuGaO_2$-EG) with high SSAs. For example, for batches needed to prepare $CuGaO_2$−P123 photocathodes, we obtained dispersed results and finally an average SSAs only slighly higher to those of $CuGaO_2$-EG (26 vs 22 m^2/g).

As the use of P-123 to produce lower $CuGaO_2$ particle size may turn out to be successful, we tried naturally to synthezise nanoparticles of Mg doped $CuGaO_2$ compound with the same technique in order to increase the conductivity of these particles and the density of charge carriers. X-ray diffraction (XRD) patterns of $CuGaO_2$:1%Mg, $CuGaO_2$:5%Mg, and $CuGaO_2$:10%Mg samples are depicted in Figure 1b. At first glance, all of the samples exhibit similar diffraction patterns than that of $CuGaO_2$-EG. A clear decrease of crystallite size (if microstrains associated with the Mg/Ga substitution are omitted) and an overall reduction of the particles size is observed on going from $CuGaO_2$-EG to $CuGaO_2$:1%Mg as illustrated by the scanning electron microscopy photographs. In fact, as shown in Figure 1a, $CuGaO_2$:1%Mg exhibits similar particle sizes as the best $CuGaO_2$−P123 sample (SSA of 43 m^2/g) with a synthesis route which turns out to be fully reproducible. For higher Mg content ($p \geq 5$), the crystallite size continues to diminish which goes along with a increase of SSA (mean SSA ∼ maximum SSA = 48 and 55 m^2/g for 5% and 10% Mg for instance). However, two extra XRD peak shoulders then show up on the powder patterns (see asterisk at ∼32° and 64° in 2θ in Figure 1b). Attempts to account for these extra peaks via the occurrence of a side product never succeeded. We concluded that $CuGaO_2$:p%Mg ($p \geq 5$) materials crystallize in a not yet identified derivative structure of $CuGaO_2$-3R.

In order to confirm the insertion of Mg in our doped samples, we have performed induced coupled plasma/optical emission spectroscopy (ICP-OES) on $CuGaO_2$−P123 and $CuGaO_2$:Mg samples. Table 1 presents the results of these analyses. First, they confirm the presence of Mg in all doped compounds. Second, the experimental Mg ratio is observed to be in good agreement with the nominal Mg ratio for 1 and 5% but lower for 10%. This suggests a limit of Mg insertion in $CuGaO_2$ under the used synthetic conditions. More striking, our analyses reveal that $CuGaO_2$:5%Mg and $CuGaO_2$:10%Mg exhibit a clear Cu deficiency. For instance, these analyses yield $Cu_{0.86}Ga_{0.953}Mg_{0.047}O_2$ and $Cu_{0.844}Ga_{0.945}Mg_{0.055}O_2$ compositions for $CuGaO_2$:5%Mg and $CuGaO_2$:10%Mg, against $CuGaO_2$ and $CuGa_{0993}Mg_{0.007}O_2$ for $CuGaO_2$−P123 and $CuGaO_2$:1%Mg, respectively. Consequently, we may speculate that the Mg^{2+}/Ga^{3+} substitution reinforces first the preexisting Cu^+/Cu^{2+} mixed valence expected in p-type $CuGaO_2$, and second the amount of copper vacancies beyond a given substitution rate estimated around 5%. Thus, two formal regimes could be discriminated that could be illustrated by the $Cu^+_{1-x}Cu^{2+}_xGa^{3+}_{1-x}Mg^{2+}_xO_2$ (low Mg doping) and $Cu^+_{1-x-2y}Cu^{2+}_{x+y}\square_yGa^{3+}_{1-x}Mg^{2+}_xO_2$ (high Mg doping) chemical formula where the symbol □ schematizes a Cu vacancy. These Cu vacancies might be responsible for the X-ray diffraction peak shoulders appearing in the powder pattern of $CuGaO_2$:5%Mg and $CuGaO_2$:10% in Figure 1b in relation with slight structural changes (with possible change of the space group) occurring beyond a given threshold.[27]

In order to evidence a signature of these vacancies in $CuGaO_2$:5%Mg, we have examined the nanoparticles by high resolution transmission electron microscopy. The micrograph in Figure 2a evidences that the nanoparticles are around 5 nm thick stacked lamellas with a structure type in good agreement with the 3R polytype (see the simulation in Figure 2b). However Figure 2, panels c and d, clearly highlights defects such as lamella curvature and twinnings. The existence of such defects could easily account for the aforementioned peak shoulders. Attempts to simulate the XRD pattern of $CuGaO_2$:5%Mg on the basis of this assumption is out of the scope of the present study. Nevertheless, we may suggest that the faulted structure observed for high Mg doping results from changes in the coordination of copper (shift of cupric ions from linear coordination to tetrahedra or octahedral environment) inducing perturbation in the long-range AABBCC stacking of oxygen spheres.

To sum up, the use of the templating agent P-123 made possible the nanostructuration of doped and undoped $CuGaO_2$ materials. At this step, we may then wonder whether these

dx.doi.org/10.1021/jp407233k | J. Phys. Chem. C 2014, 118, 54−59

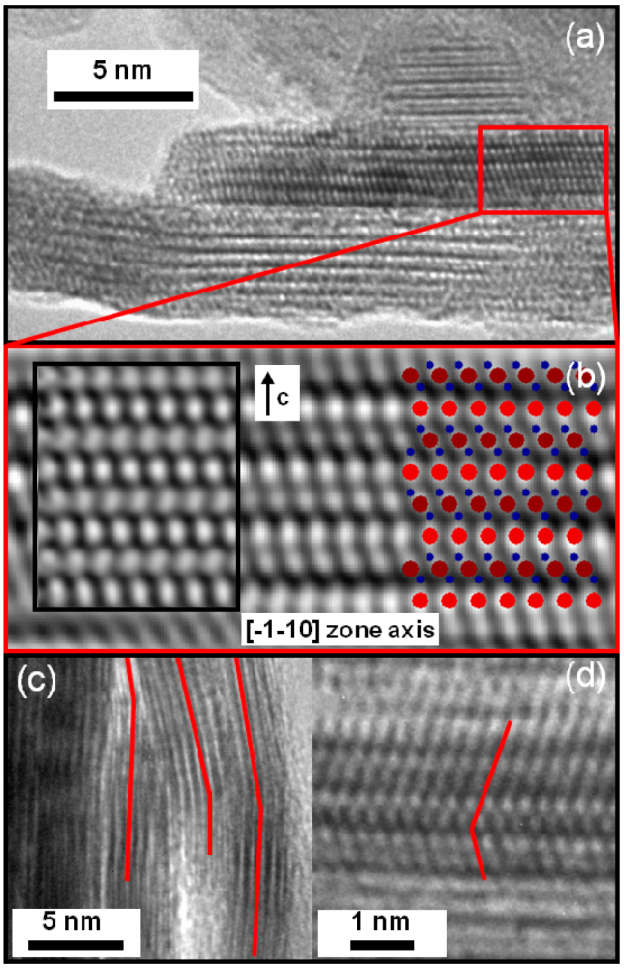

Figure 2. TEM micrographs of $CuGaO_2$:5%Mg. (a) Stacked lamellas and (b) enlargement of the region marked by a red rectangle in panel a. Left: simulation[28] of 3R $CuGaO_2$ along [−1−1 0] axis. Right: corresponding structural model (blue, oxygen; red, copper; brown, gallium). (c) Curved lamellas and (d) twins.

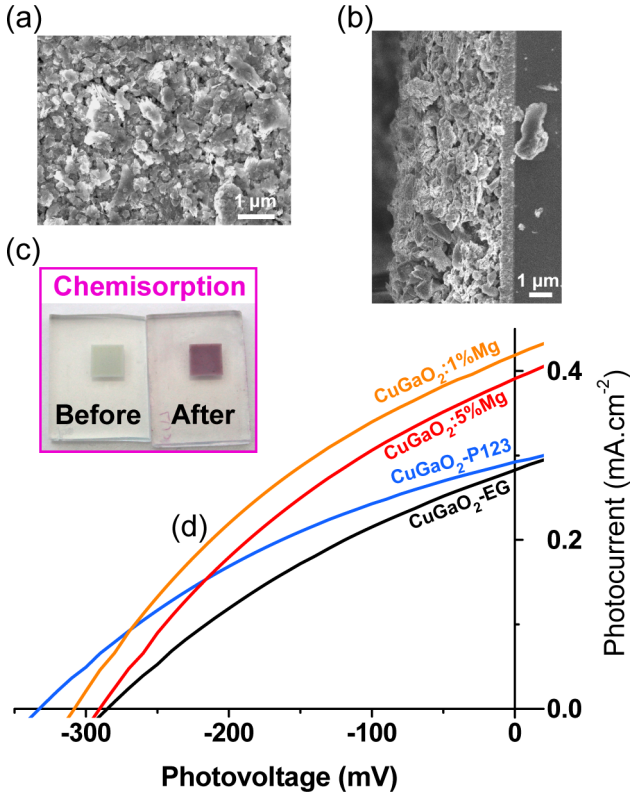

Figure 3. (a) Top and (b) side views of $CuGaO_2$:1%Mg film observed by scanning electron microscopy after sintering at 350 °C in air. (c) Photographs of the $CuGaO_2$:1%Mg electrode before and after chemisorption of the PMI-NDI dye at the surface. (d) Photoresponse under AM1.5 illumination of solar cells made of $CuGaO_2$-EG, $CuGaO_2$, $CuGaO_2$:1%Mg, and $CuGaO_2$:5%Mg.

Table 2. Photovoltaic Performances of DSSCs Based on $CuGaO_2$-EG, $CuGaO_2$, $CuGaO_2$:1%Mg, and $CuGaO_2$:5%Mg

	V_{OC} (mV)	J_{SC} (mA cm^{-2})	FF (%)	η (%)
$CuGaO_2$:5%Mg	295	0.387	33	0.038
$CuGaO_2$:1%Mg	305	0.415	35	0.045
$CuGaO_2$−P123	335	0.290	35	0.034
$CuGaO_2$-EG	285	0.280	33	0.026

samples exhibit higher photovoltaic properties than $CuGaO_2$-EG, our reference sample. In that respect, DSSCs were prepared from $CuGaO_2$−P123, $CuGaO_2$:1%Mg, and $CuGaO_2$:5%Mg samples, and their photovoltaic performances were tested. $I-V$ characteristics, as well as views of a $CuGaO_2$:1%Mg film, are depicted in Figures 3a−d. The parameters are compiled in Table 2. As opposed to previous investigations, 4 μm thick crack free films were prepared here by screen-printing, a much more reproducible technique than doctor blading[4] or dropping.[5] Of course, all of these deposition techniques may lead to different FTO/SC interfaces. For this reason, photovoltaic results collected via these different coating methods are not fully comparable. In that context, we have also prepared $CuGaO_2$-EG photocathodes by screen printing according to the same route. Clearly, from data collected in similar conditions with identical dye and mediator, the conversion efficiency increases from $CuGaO_2$-EG (0.026%) to $CuGaO_2$−P123 (0.034%). Surprisingly, this increase in performance seems to be mainly due to an increase of *Voc* rather than an expected increase of J_{SC} related to an increase of SSA and consequently of dye loading. On the other hand, an important increase of J_{SC} is observed for $CuGaO_2$:1%Mg that exhibits a conversion efficiency (0.045%) more than 70% higher than for $CuGaO_2$-EG. This increase of J_{SC} may be viewed as mainly driven by the enhancement of the SSA (and dye loading) under doping (see Figure 4). Conversely, this trend is reversed for higher Mg doping. Indeed, going from $CuGaO_2$:1%Mg to $CuGaO_2$:5%Mg, the efficiency is reduced from 0.045% to 0.038%. This result is puzzling as, the efficiency being a priori correlated to the surface specific area, we could anticipate that a strong enhancement of the SSA from $CuGaO_2$:1%Mg to $CuGaO_2$:5%Mg would cause a higher light harvesting efficiency via an increase of chemisorbed dye concentration. This is effectively what is observed from dye absorption measurements (Figure 4) but surprisingly this does not result in higher photocurrent. We may infer that highly doped $CuGaO_2$ nanoparticles have a lower conductivity than sligthly doped nanoparticles. Indeed, a large concentration of Mg dopant induces Cu deficiencies which might scatter the photoinjected charges and then limit their mean free path and subsequently the charge flow in the photocathode. Overall, our results indicate clearly that the conductivity as well as the nanostructuration of the $CuGaO_2$ particles plays an important role in the efficiency of $CuGaO_2$ photocathodes.

dx.doi.org/10.1021/jp407233k | J. Phys. Chem. C 2014, 118, 54−59

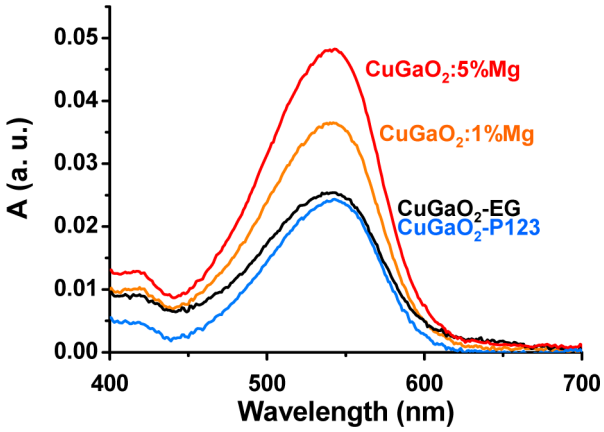

Figure 4. Absorption spectra of desorbed PMI-NDI dye issued from photocathodes based on $CuGaO_2$-EG, $CuGaO_2$–P123, $CuGaO_2$:1% Mg, and $CuGaO_2$:5%Mg.

CONCLUSION

We have explored a new synthetic route of $CuGaO_2$ nanoparticles with P123 polymer as templating agent and redox Cu^+ stabilizator in aqueous solution. This led to a significant enhanced specific surface areas compared to previous investigations. Nevertheless, this chemical route suffers yet from a lack of reproducibility, i.e. SSA vary in a large range. Fortunately, extrapolations of this protocol to the preparation of $CuGaO_2$:Mg to generate a larger amount of hole carriers yielded large specific surface areas (e.g., 43 and 48 m^2/g for $CuGaO_2$:1%Mg and $CuGaO_2$:5%Mg) in a very reproducible manner. DSSCs were then assembled with PMI-NDI dyad as dye and a tris(4,4′-bis-tert-butyl-2,2′-bipyridine)cobalt(II/III) based electrolyte and yield conversion efficiencies similar to those commonly reported for NiO. For $CuGaO_2$:1%Mg, an increase of 73% in photovoltaic yield is observed compared to undoped $CuGaO_2$-EG initially prepared according to Srinivasan et al.[18] It is worth noticing that the higher performances are not achieved for the more nanostruturated and doped $CuGaO_2$ materials, i.e., $CuGaO_2$:5%Mg (and a fortiori $CuGaO_2$:10% Mg), most likely due to a too large content of structural defects limiting the charge flow and favoring electron–hole recombination at the SC–dye interface. Consequently, $CuGaO_2$ confirms its status as a potential substitute of NiO even if many investigations still have to be carried out to compete with very recent NiO–DSSCs with very high photoconversion efficiency.

AUTHOR INFORMATION

Corresponding Authors

*E-mail: Laurent.cario@cnrs-imn.fr. Tel: 33.2.40.37.39.88.
*E-mail: stephane.jobic@cnrs-imn. Tel: 33.2.40.37.39.22.

Author Contributions

The manuscript was written through contributions of all authors. All authors have given approval to the final version of the manuscript.

Notes

The authors declare no competing financial interest.

ACKNOWLEDGMENTS

The authors thank the “Région Pays de la Loire” and the agency ANR-Progelec for financial support via the programs PERLE2 and POSITIF (No. ANR-12-PRGE-0016-01), respectively.

REFERENCES

(1) Le Pleux, L.; Chavillon, B.; Pellegrin, Y.; Blart, E.; Cario, L.; Jobic, S.; Odobel, F. Simple and Reproducible Procedure to Prepare Self-nanostructured NiO Films for the Fabrication of p-type Dye-sensitized Solar Cells. *Inorg. Chem.* **2009**, *48*, 8245–8250.
(2) Sumikura, S.; Mori, S.; Shimizu, S.; Usami, H.; Suzuki, E. Photoelectrochemical Characteristics of Cells with Dyed and Undyed Nanoporous p-type Semiconductor CuO Electrodes. *J. Photochem. Photobiol., A* **2008**, *194*, 143–147.
(3) Nattestad, A.; Zhang, X.; Bach, U.; Cheng, Y.-B. Dye-sensitized $CuAlO_2$ Photocathodes for Tandem Solar Cell Applications. *J. Photon. Energy* **2011**, *1*, 011103/011101–011103/011109.
(4) Renaud, A.; Chavillon, B.; Le Pleux, L.; Pellegrin, Y.; Blart, E.; Boujtita, M.; Pauporté, T.; Cario, L.; Jobic, S.; Odobel, F. $CuGaO_2$: a Promising Alternative for NiO in p-type Dye Solar Cells. *J. Mater. Chem.* **2012**, *22*, 14353–14356.
(5) Yu, M.; Natu, G.; Ji, Z.; Wu, Y. p-type Dye-Sensitized Solar Cells Based on Delafossite $CuGaO_2$ Nanoplates with Saturation Photovoltages Exceeding 460 mV. *J. Phys. Chem. Lett.* **2012**, *3*, 1074–1078.
(6) Xiong, D.; Xu, Z.; Zhang, W.; Chen, W.; Xu, X.; Wang, M.; Cheng, Y.-B. Hydrothermal Synthesis of Ultrasmall $CuCrO_2$ Nanocrystal Alternatives to NiO Nanoparticles in Efficient p-type Dye-Sensitized Solar Cells. *J. Mater. Chem.* **2012**, *22*, 24760–24768.
(7) Odobel, F.; Pellegrin, Y.; Gibson, E. A.; Hagfeldt, A.; Smeigh, A. L.; Hammarström, L. Recent Advances and Future Directions to Optimize the Performances of p-type Dye-Sensitized Solar Cells. *Coord. Chem. Rev.* **2012**, *256*, 2414–2423.
(8) O'Regan, B.; Grätzel, M. A Low-Cost, High-Efficiency Solar Cell Based on Dye-Sensitized Colloidal TiO_2 Films. *Nature* **1991**, *353*, 737–740.
(9) Keis, K.; Magnusson, E.; Lindstrom, H.; Lindquist, S. E.; Hagfeldt, A. A 5% Efficient Photoelectrochemical Solar Cell Based on Nanostructured ZnO Electrodes. *Sol. Energ. Mater. Sol. C* **2002**, *73*, 51–58.
(10) He, J.; Lindström, H.; Hagfeldt, A.; Lindquist, S.-E. Dye-Sensitized Nanostructured p-type Nickel Oxide Film as a Photocathode for a Solar Cell. *J. Phys. Chem. B* **1999**, *103*, 8940–8943.
(11) He, J.; Lindström, H.; Hagfeldt, A.; Lindquist, S.-E. Dye-Sensitized Nanostructured Tandem Cell-First Demonstrated Cell with a Dye-Sensitized Photocathode. *Sol. Energ. Mater. Sol. C* **2000**, *62*, 265–273.
(12) Odobel, F.; Le Pleux, L.; Pellegrin, Y.; Blart, E. New Photovoltaic Devices Based on the Sensitization of p-type Semiconductors: Challenges and Opportunities. *Acc. Chem. Res.* **2010**, *43*, 1063–1071.
(13) Nattestad, A.; Mozer, A. J.; Fischer, M. K.R.; Cheng, Y.-B.; Mishra, A.; Bäuerle, P.; Bach, U. Highly Efficient Photocathodes for Dye-Sensitized Tandem Solar Cells. *Nat. Mater.* **2010**, *9*, 31–25.
(14) Huang, Z.; Natu, G.; Ji, Z.; He, M.; Yu, M.; Wu, Y. Probing the Low Fill Factor of NiO p-type Dye-Sensitized Solar Cells. *J. Phys. Chem. C* **2012**, *116*, 26239–26246.
(15) Powar, S.; Daeneke, T.; Ma, M. T.; Fu, D.; Duffy, N. W.; Weidelener, M.; Mishra, A.; Bäuerle, P.; Spiccia, L.; Bach, U. Highly Efficient p-type Dye-Sensitized Solar Cells Based on Tris(1,2-diaminoethane)cobalt(II)/ (III) Electrolytes. *Angew. Chem.* **2013**, *125*, 630–633.
(16) Bai, J.; Xu, X.; Xu, L.; Cui, J.; Huang, D.; Chen, W.; Cheng, Y.; Shen, Y.; Wang, M. Potassium-doped Zinc Oxide as Photocathode Material in Dye-Sensitized Solar Cells. *ChemSusChem.* **2013**, *6*, 622–629.
(17) Xiong, D.; Zhang, W.; Zeng, X.; Xu, Z.; Chen, W.; Cui, J.; Wang, M.; Sun, L.; Cheng, Y.-B. Enhanced Performance of p-type Dye-Sensitized Solar Cells Based on Ultrasmall Mg-doped $CuCrO_2$ Nanocrystals. *ChemSusChem* **2013**, *6*, 1432–1437.
(18) Srinivasan, R.; Chavillon, B.; Doussier-Brochard, C.; Cario, L.; Paris, M.; Gautron, E.; Deniard, P.; Jobic, S. Tuning the Size and Color

of the p-type Wide Band Gap Delafossite Semiconductor $CuGaO_2$ with Ethylene Glycol Assisted Hydrothermal Synthesis. *J. Mater. Chem.* **2008**, *18*, 5647−5653.
(19) Nattestad, A.; Ferguson, M.; Kerr, R.; Cheng, Y.-B.; Bach, U. Dye-Sensitized Nickel(II) Oxide Photocathodes for Tandem Solar Cell Applications. *Nanotechnology* **2008**, *19*, 295304/1−295304/9.
(20) Kavan, L.; Yum, J.-H.; Graetzel, M. Optically Transparent Cathode for Co(III/II) Mediated Dye-Sensitized Solar Cells Based on Graphene Oxide. *ACS Appl. Mater. Interfaces* **2012**, *4*, 6999−7006.
(21) Hao, F.; Dong, P.; Luo, Q.; Li, J.; Lin, H. Recent Advances in Alternative Cathode Materials for Iodine-Free Dye-Sensitized Solar Cell. *Energy. Environ. Sci.* **2013**, *6*, 2003−2019.
(22) Gibson, E. A.; Smeigh, A. L.; Pleux, L. L.; Fortage, J.; Boschloo, G.; Blart, E.; Pellegrin, Y.; Odobel, F.; Hagfeldt, A.; Hammarström, L. A p-type NiO-Based Dye-Sensitized Solar Cell with an Open-Circuit Voltage of 0.35 V. *Angew. Chem., Int. Ed.* **2009**, *48*, 4402−4405.
(23) Cabo, M.; Pellicer, E.; Rossinyol, E.; Solsona, P.; Castell, O.; Suriñach, S.; Baro, M. D. Influence of the preparation method on the morphology of templated $NiCo_2O_4$ spinel. *J. Nanopart. Res.* **2011**, *13*, 3671−3681.
(24) Zhang, R.; Dai, H.; Du, Y.; Zhang, L.; Deng, J.; Xia, Y.; Zhao, Z.; Meng, X.; Liu, Y. P123-PMMA Dual-Templating Generation and Unique Physicochemical Properties of Three-Dimensionally Ordered Macroporous Iron Oxides with Nanovoids in the Crystalline Walls. *Inorg. Chem.* **2011**, *50*, 2534−2544.
(25) Koehler, B. U.; Jansen, M. Darstellung und Strukturdaten von ″Delafossiten″ $CuMO_2$ (M= Al, Ga, Sc, Y). *Z. Anorg. Allg. Chem.* **1986**, *543*, 73−80.
(26) Ueda, K.; Hase, T.; Yanagi, H.; Kawazoe, H.; Hosono, H. Epitaxial Growth of Transparent p-type Conducting $CuGaO_2$ Thin Films on Sapphire (001) Substrates Pulsed Laser Deposition. *J. Appl. Phys.* **2001**, *89*, 1790−1793.
(27) The possible existence of Cu vacancies in high Mg doped $CuGaO_2$ materials is supported by unpublished syntheses of undoped "$CuGaO_2$" prepared according to the chemical route reported here but with sodium acetate/ acetic acid as buffer solution. Pure materials with identical XRD patterns than those of $CuGaO_2$:5%Mg and $CuGaO_2$:10%Mg were then obtained with a Cu:Ga atomic ratio determined by energy dispersive X-ray spectroscopy of 0.8 (against 1.0 for $CuGaO_2$-P123) and a density of 5.90 (against 6.21 for $CuGaO_2$-P123).
(28) Koch, C. T. Determination of Core Structure Periodicity and Point Defect Density along Dislocations; *Ph.D. Thesis*, Arizona State University: Phoenix, AZ, 2002.